Research Article

Eco-friendly approach to control dengue vector *Aedes aegypti* larvae with their enzyme modulation by *Lumnitzera racemosa* fabricated zinc oxide nanorods

Pratik P. Dhavan[1] · **Bhaskar L. Jadhav**[1]

Received: 8 December 2019 / Accepted: 30 March 2020 / Published online: 7 April 2020

Abstract

Aedes aegypti mosquito species is a primary vector for dengue, chikungunya and Zika infections, and vector control is the only key approach for reducing their transmission. The present study emphasizes on environmental friendly approach for the fabrication of zinc oxide nanorods (ZnO NRs) using aqueous extract of *Lumnitzera racemosa* flower buds (LB) as a reducing and stabilizing agent. ZnO NRs were examined by UV–Vis spectroscopy with characteristic absorbance band at 373.82 nm and bandgap of 3.25 eV. FT-IR analysis revealed the functional groups associated with ZnO NRs. The crystallinity of LB-ZnO NRs was further investigated using X-ray diffraction. The Zeta potential displayed a surface charge of − 23.5 mV on NRs. Energy dispersive spectra analysis and SEM analysis confirmed the formation of ZnO NRs whilst TEM highlighted the average length and diameter in the range of 250–300 nm and 45–50 nm respectively. LB-ZnO NRs were found to be efficacious against *Ae. aegypti* 4th instar larvae with LC_{50} of 24.74 µg/ml. Decreased acetylcholinesterase (60.6%) and glutathione S-transferase (24.4%) activities were also evaluated in *Ae. aegypti* larvae which were exposed to synthesized LB-ZnO NRs with no genetic aberrations. All these outcomes propose the potential employment of LB-ZnO NRs in mosquito control, as well as an effective alternative to insecticide resistance.

Graphical abstract

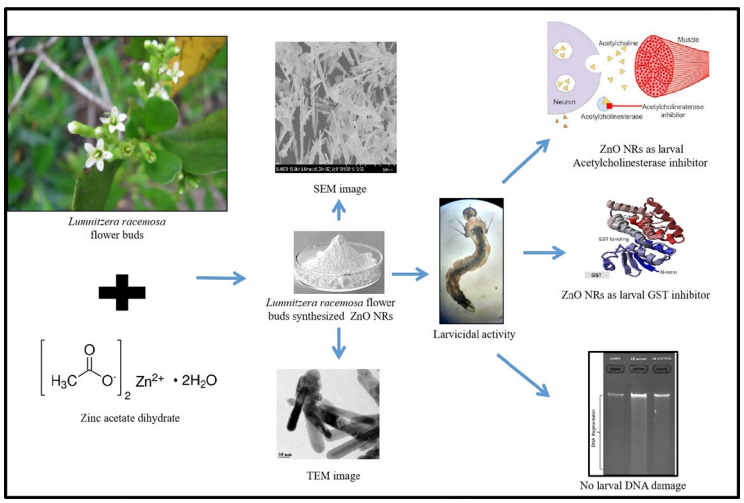

✉ Pratik P. Dhavan, pratik.dhavan11@gmail.com; Bhaskar L. Jadhav, drbljadhav@gmail.com | [1]Department of Life Sciences, University of Mumbai, Vidyanagari campus, Santacruz (East), Mumbai 400098, India.

SN Applied Sciences (2020) 2:843 | https://doi.org/10.1007/s42452-020-2636-0

Keywords *Aedes aegypti* · Green synthesis · *Lumnitzera racemosa* · ZnO nanorods · Mosquito-larvicidal

1 Introduction

Arthropods are hazardous vectors that could influence the growing global human and animal population as epidemics and pandemics of lethal pathogens [1]. The most important threats faced by mosquitoes worldwide are those (Diptera: Culicidae), which are the vectors of important diseases such as yellow fever, Western Nile virus (WNV), dengue, malaria and filariasis. Millions of individuals globally are at risk and endangering life due to mosquito-borne illnesses, and have such a heavy public health burden that they are blamed on continuous continental underdevelopment [2].

The knowledge about ecology and the control of mosquitoes is of crucial importance in the sense of integrated vector management, to combat the spread of many mosquito-borne diseases [3, 4]. *Ae. aegypti* (Linnaeus) is the primary dengue and Zika vector, a cosmotropic species. As a vector of dengue fever and chikungunya in India, this species is particularly dangerous because the number of dengue fever instances has increased substantially over the past years [1, 5, 6]. Chemical insecticides used for regulating mosquitoes which are detrimental to human health and non-target organisms. Moreover, mosquito vectors have developed resistance towards the synthetic insecticides, namely temephos by carrying genes that encode acetylcholinesterases (AChE). AChE enzyme breaks down acetylcholine which carries the transmission of nerve impulses through the synaptic gap and acts as a primary target for synthetic insecticides [7]. Besides, a detoxifying enzyme such as Glutathione S-transferase (GST) is also expressed by insects which helps to neutralize the toxicity of different xenobiotics [8]. On these grounds, newly implemented eco-friendly methods have been used to improve mosquito vector control [9]. Young mosquito instars have shown decreased mobility and are therefore often easy to target. Thus mosquitoes can be killed before dispersing to human dwellings by targeting at their larval stages [10].

Plant materials showing mosquitocidal characteristics against major mosquito vectors have been recently emphasized. Many naturally occurring compounds isolated from plants exhibits excellent mosquito toxicants which act as ovicidal, pupicidal, adult repellents, growth and/or breeding inhibitors [11]. *Lumnitzera racemosa* Willd. (Combretaceae) is a true mangrove found along the coast of Asia. Due to the high calorific value, the wood of *L. racemosa* is used as a fuel, while its leaves are eaten on South Pacific Island all through periods of scarcity by herbivores [12]. Besides, the reddish bark contains ~ 15 × 19% tannins used in leather industries. Moreover, fluid extracted from the stem of this plant were found effective in treating itches and herpes when applied externally. The most important secondary metabolites of *L. racemos*a are flavonoids, triterpenoids, tannins, fatty acids and polyisoprenoid alcohols [13]. This plant exerts numerous pharmacological activities, such as antibacterial [14], antifungal and antihypertensive [15], protein tyrosine phosphatase 1B (PTP1B) inhibitory, hepatoprotective and antioxidant activities [16]. While recent studies revelled *L. racemosa* leaves to be toxic against larvae of *Ae. aegypti* [17].

Green technologies have recently been shown to be a new strategy for reducing the use of chemical pesticides since overuse has often led to massive non-target impacts and widespread resistance [9, 18]. Modern study has revealed an increased level of insecticide activity in green nanoparticles (NPs) synthesized by *Euphorbia rothiana* [19], *Cymbopogon citratus* [20], *Pedalium murex* [21] etc. Among different NPs, Zinc Oxide nanoparticles (ZnO NPs), having nanosized morphology, have increased interest among several researchers as a result of their exclusive optical or chemical activities [22]. ZnO NPs have remarkable characteristics, including large binding energy, broad bandgap, and elevated piezoelectric characteristics [23]. It has various applications, including UV light-emitting diodes, laser diodes, and catalysts [24]. Also, ZnO NPs have a highly promising prospect for biological functions such as gene delivery [25], biological sensing and labelling [26], drug delivery and nanomedicine [27, 28], antibacterial [29], antifungal [30], along with larvicidal, acaricidal, pediculicidal activity [31].

The present study was thus focussed on ZnO Nanorods (ZnO NRs) synthesis with a single step procedure based on easy to obtain *L. racemosa* flower buds aqueous extract. LB-ZnO NRs were characterized using a variety of biophysical methods. Furthermore, larvicidal toxicity of LB extract and LB-ZnO nanorods were evaluated on dengue vector *Ae. aegypti* and their enzyme modulation on AChE and GST enzymes were studied.

2 Materials and methods

2.1 Materials and reagents

Lumnitzera racemosa flower buds (LB) were collected from Bhatye beach area located at 16°58′44.0691″ N and 73°17′38.7499″ E. Ratnagiri District, Maharashtra, India and authenticated by an expert taxonomist. *L. racemosa*

flower buds were washed thoroughly with tap water followed by distilled water to remove adhered particles. Flower buds were then kept for drying under the shade at room temperature (27 ± 2 °C). Water purified using Millipore Milli-Q (18.2 MΩ.cm at 25 °C) purification system was used throughout the experiment. Acetylthiocholine iodide was purchased from Hi-Media (Mumbai, India), reduced glutathione (GSH), 1-chloro2,4-dinitrobenzene (CDNB), DTNB reagent (5,5′-dithiobis-2-nitrobenzoic acid), Zinc acetate dihydrate, Agarose, Ethylenediaminetetraacetic acid (EDTA) and ethidium bromide were purchased from Sigma-Aldrich, India. Proteinase K and RNase A were procured from ThermoFisher Scientific, India.

2.1.1 Preparation of *L. racemosa* flower buds extract

Aqueous LB extract was prepared by adding 5 gm plant powder in 100 ml Milli-Q water (MQ-W) and placed in a water bath at 100 °C for 20 min. The obtained filtrate and residue were separated using Whatman filter paper No. 42 (42 ashless diameters 125 mm GE Healthcare Life Sciences). Filtrate solution thus obtained is filtered with a 0.2 µm cellulose syringe filter (Rayna Biotech, UK) and stored in the refrigerator at 4 °C and was later used for the synthesis of ZnO NPs.

2.1.2 Production of zinc oxide nanoparticles

To 80 ml of 10 mM zinc acetate dihydrate, 20 ml of obtained LB aqueous extract was added dropwise under constant stirring at room temperature. The resulting solution was then placed on a magnetic stirrer at 60 °C until the off-white suspension of NPs were formed. The solution was then centrifuged at 3000 rpm for 20 min and the residue was washed several times to remove any unreacted materials. The resulting supernatant was discarded, and the pellet was collected and placed in a furnace at 400 °C to obtain the desired product in powder form.

2.2 Characterization

2.2.1 UV–Vis spectroscopy (UV–Vis)

Optical properties of nanoparticles were examined using UV–Vis spectroscopy. Absorption spectrum of ZnO NPs after 24 h was recorded using UV–Visible spectrometer Shimadzu, UV-1800 (λ = 200–800 nm) to confirm the synthesis of LB-ZnO NPs.

2.2.2 Fourier transform infrared spectroscopy (FTIR)

Different types of functional groups which are associated with the synthesis of NPs was confirmed through FTIR analysis. The dried powder of ZnO NPs was thoroughly mixed with potassium bromide (KBr) (2:98 ratio w/w) and compressed at 11,000 psi to make the disc. The disk was then inserted into the FTIR spectrophotometer (Perkin Elmer Frontier, 91579) and the spectrum was recorded at the diffuse reflection mode at a resolution of 4 cm^{-1} in the test range of 500–4000 cm^{-1}. A similar process with LB aqueous extract was also performed.

2.2.3 X-ray diffraction (XRD)

Crystalline nature of synthesized LB-ZnO NPs was recorded using XRD diffraction working at 40 kV with a current of 40 mA, Cu Kα radiation (1.54 Å) in a θ–2θ configuration using Bruker D8 Discover model (Bruker, Germany).

2.2.4 Scanning electron microscopy (SEM) and Energy-dispersive spectra (EDS)

Scanning electron microscopes (SEM) helps in the validation of NPs morphology. A few micrograms of LB-ZnO NPs were dropped on a carbon-coated copper grid for SEM analysis and the excess powder was discarded. The scanning electron microscopic images were then captured using JEOL System JSM-6390LV (Akishima, Tokyo, Japan) at an acceleration voltage of 15 kV. An energy dispersive spectrometer (EDS make FEI series Quanta 200 with EDS 3.0.13) at an energy range of 0–10 keV was used to take energy dispersive spectra for LB-ZnO NPs.

2.2.5 Zeta potential

Zeta potential was performed to analyze charge on synthesized LB-ZnO NPs using Zetasizer (Nano series Nano-ZS90, Malvern Instruments).

2.2.6 Transmission electron microscopy (TEM)

On carbon-coated copper grids, powdered LB-ZnO NPs were mounted and transmission electron microscopy observations were carried out using FEI Tecnai G2, F30 system working at an accelerating voltage of 200 kV.

2.3 Mosquito rearing and larvicidal activity

The larvae of *Ae. aegypti* were collected from Vidyanagari campus, University of Mumbai, Kalina, Mumbai, and surrounding areas. Collected larvae were identified by Dr. Mira Ramaiya, Entomologist, Haffkine Institute For Training, Research And Testing, Parel, Mumbai. The larval colony was maintained in the lab at 28 ± 1 °C with 80 ± 5% relative humidity, and 14L:10D photoperiod [32]. Adults were fed with 2% sucrose solution soaked in non-absorbent cotton.

Female mosquitoes were fed with periodic blood meals for egg maturation by the membrane feeding technique [33]. The eggs were collected on Whatman filter paper lined in the bowl and allowed to hatch in dechlorinated water. A 2:1 (w/w) mixture of yeast powder and dog biscuits were used to feed the larvae. The pupae formed were gathered and moved to glass cages for adult emergence. Laboratory colonies of mosquito larvae (F1 generation) were used for the larvicidal activity.

Larvicidal activity of LB aqueous extract and synthesized LB-ZnO NPs was carried out under the WHO standard method [34] as follows. Accordingly, LB extract and LB-ZnO NPs were dispersed in dechlorinated water to prepare a graded series of concentration (500–2500 µg/ml, for aqueous LB extract and 10–50 µg/ml, for LB-ZnO NPs). Further, early 4th instar larvae of *Ae. aegypti* were transferred to 250 ml plastic cups in batches of 20 each containing 199 ml of distilled water and 1 ml of respective treatment in the graded concentrations. Each experiment was conducted in triplicates along with a respective control group on three separate days to ensure reproducibility. The control group consisted of 200 ml of distilled water only. No food was provided during the duration of the entire experiment. Symptoms of the treated larvae and larval mortality were assessed by observing their motility 24 h after exposure to their respective treatments.

2.3.1 Photomicrography studies

Studies of photomicrography were conducted with minor modifications based on Coelho et al. [35] methodology. Morphological alterations were checked in the 4th instar larvae of *Ae. aegypti* treated with LB extract and LB-ZnO NPs at their median lethal concentrations (LC_{50}) along with the control group. The treatment groups (LB, LB-ZnO NPs) and control larvae were successively fixed at 27 °C for 30 min in alcohol (ethanol) dehydration (35–70%) and placed on glass slides. The larvae were analyzed under the Stereo zoom microscope (Leica microsystems) at ×20 magnification.

2.4 Enzymatic studies

To study the neurotoxicity and the effect of detoxification on *Ae. aegypti* larvae separate studies were conducted to analyze the effect of LB extract and LB synthesized ZnO NPs on AChE and GST enzymes. Early 4th instar larvae were exposed for 24 h to LB extract and ZnO NPs at their median lethal concentrations (LC_{50}). It is advantageous to study the effect of a toxicant on the organism at the moment of evaluation but before mortality occurred. Accordingly, only the live larvae recovered after 24 h from both control and treated with LB extract and LB-ZnO NPs were used for further biochemical analysis.

2.4.1 Preparation of whole-body homogenates for assessment of enzyme activity

The larvae were retrieved after 24 h of treatment with LB aqueous extract and ZnO NPs (test larvae) alongside with untreated (control larvae) and washed with double distilled water accompanied by blotting their body surface with tissue paper to eliminate any contaminants. The collected larvae were then homogenized with a Teflon hand homogenizer in 0.5 ml phosphate buffer [100 mM phosphate buffer (pH 7.2) and 1% Triton X-100] in Eppendorf ™ tubes (submerged in ice) [36]. The homogenate was centrifuged at 10,000×*g* for 15 min at 4 °C, and the supernatant was used to assess enzyme activity. Enzyme protein was estimated according to the Bradford method [37].

2.4.2 Acetylcholinesterase (AChE) activity

AChE activity in the whole body homogenates of larvae was spectrophotometrically measured according to a modified method of Ellman et al. [38] using acetylthiocholine iodide as a substrate [39]. 50 µl aliquot of homogenate (100 µg/ml crude enzyme) was successively mixed with 450 µl sodium phosphate buffer (100 mM, pH 7.5); 50 µl of 10 mM DTNB and 50 µl of 12.5 mM acetylcholine iodide. After 5 min of incubation at room temperature, the optical density of the sample was read at 400 nm using a spectrophotometer (Shimadzu, UV-1800) against a suitable reagent blank (without enzyme). AChE activity was expressed as (µmol ACT released/min/mg protein) using published extinction coefficient ($e = 1.3\ mM^{-1}\ cm^{-1}$).

2.4.3 Glutathione S-transferase (GST) activity

GST activity was estimated by Vontas et al. [40] method as follows. 100 µl of 30 mM CDNB was added to the 100 µl larval homogenate (100 µg/ml crude enzyme) and the volume was adjusted to 500 µl using sodium phosphate buffer (100 mM, pH 7.5). After pre-incubation of the reaction mixture at 37 °C for 5 min, 100 µl of 30 mM of GSH was added. The change in the absorbance level was noted at 340 nm for 5 min after every 1 min interval in the spectrophotometer. The reaction mixture without enzyme was used as blank. GST activity was expressed as (µmol CDNB hydrolysed /min/mg protein) using the published extinction coefficient ($e = 9.6\ mM^{-1}\ cm^{-1}$) [41].

2.5 DNA fragmentation assay

To analyze any damage caused by LB extract and LB-ZnO NPs on mosquito DNA, fragmentation analysis was carried out as per established protocol [42]. Mosquito larvae treated with plant extract and ZnO NRs were washed with ethanol, distilled water to remove adhered particles. Larvae were lysed in a 250 µl cell lysis buffer containing 50 mM Tris–HCl, 0.5% SDS, 1 µg/ml proteinase K (pH 8.0), 10 mM of ethylenediaminetetraacetic acid (EDTA) and RNase A (0.5 µg/ml) at 37 °C. DNA was extracted by phenol/chloroform/isoamyl alcohol (25:24:1) method [43]. The 260/280 nm absorbance ratio was used to assess the purity of DNA [44]. Electrophoresis of larval DNA was performed on an agarose gel (1%) containing ethidium bromide (1 µg/ml) at 100 V, and the fragments of DNA were visualized by exposing the gel to UV light and photographed on Gel documentation system (Bio-Rad Gel Doc XR system).

2.6 Statistical data analysis

The data acquired were analyzed using the SPSS 21.5 program for regression analysis. The values of LC_{50} and LC_{90} with 95% fiducial limits and chi-square were calculated using Probit analysis in each bioassay. The data were expressed as Mean ± SEM. One-way variance analysis (ANOVA) followed by the post-hoc Tuckey test was performed to determine the difference in enzyme inhibition between control and treated groups. Results with $p < 0.05$, were considered to be statistically significant.

3 Results and discussion

3.1 Characterization

3.1.1 UV–Visible spectroscopy

UV–vis spectroscopy is an easy and efficient method for the identification of nanoparticle formation, stabilization, and shape [45]. The UV–vis spectrum of LB-ZnO NPs synthesized using LB aqueous extract and zinc acetate is shown in Fig. 1a. During synthesis, the color of the reaction mixture changed from yellow to pale white colored precipitate. The obtained product after calcination at 400 °C gave white precipitate indicating the synthesis of ZnO NPs which was further confirmed by UV–Vis spectroscopy. A characteristic absorption peak at 373.82 nm could be attributed, due to electron transfer from the valence band to the conductive band, related to ZnO's intrinsic bandgap absorption (O2p-zn3d) [46]. In comparison to the average absorption at 377 nm of ZnO NPs, the synthesized LB-ZnO NPs with a maximum wavelength at 373.82 nm were slightly blue-shifted which maybe because of the decrease in particle size with respect to bulk ZnO [47]. Mahamuni et al. [48] and Ishwarya et al. [49] reported a similar shift in the position of the absorption peak of ZnO NPs. Figure 1b shows the optical energy bandgap (Eg) of LB-ZnO NPs which was estimated using the following Tauc formula [50].

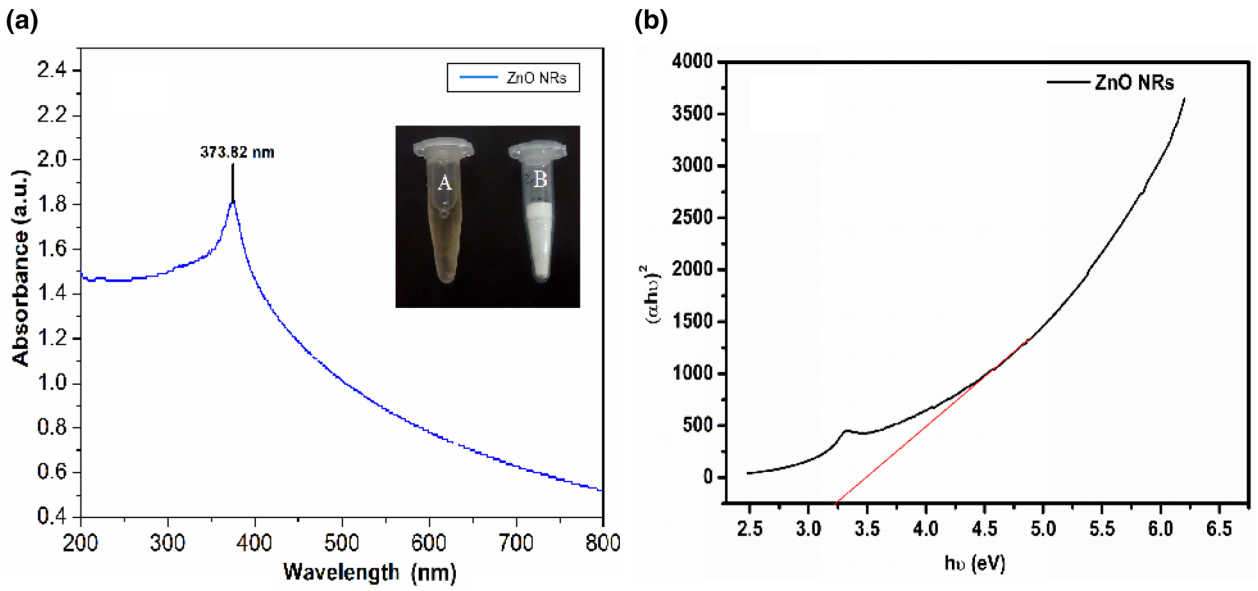

Fig. 1 **a** UV–visible absorption spectrum of zinc oxide nanoparticles synthesized using *L. racemosa* flower buds aqueous extract [Inset: (A) *L. racemosa* flower buds extract and (B) synthesized ZnO NRs]. **b** Optical energy band gap of synthesized ZnO nanorods

$$\text{Optical energy bandgap } (Eg) = \frac{hc}{\lambda} \quad (1)$$

where h and c refers to planks constant (6.626×10^{-34} J s) and velocity of light (3×10^{8} m/s) respectively and 'λ' denotes optical wavelength.

The synthesized LB-ZnO NP's optical energy band gap was found to be 3.25 eV which is in good agreement with the previous report [50]. This changes in the optical band gap of LB-ZnO NPs concerning the ZnO nanostructure morphology further confirms that nanostructure crystallinity, crystal growth facets, and crystal grain size lead to the effective band gap of nanostructured ZnO smaller than its bulk value of 3.37 eV [51].

3.1.2 FT-IR analysis

FT-IR provides data on a molecule's vibrational and linear mode of motion and is, therefore, a significant method for identifying and characterizing a material. Infrared spectrum of any compound (organic or inorganic) offers a distinctive fingerprint that is easily differentiated from all other compound's absorption patterns. The FT-IR spectrum of LB aqueous extract and synthesized LB-ZnO NPs are shown in Fig. 2a, b respectively. In Fig. 2a, spectral peak at 3291 cm^{-1} is due to O–H stretching and 2922 cm^{-1} is due to C–H stretch [52]. Absorption peak from the carbonyl group appears at 1613 cm^{-1}, whereas the band at 1235 cm^{-1} observed is due to primary amine groups and –C–O stretching mode [53]. The absorption band at 1017 cm^{-1} is due to C–N stretching oscillation mode of amines that are characteristics of proteins/enzymes [54, 55]. In Fig. 2b which corresponds to the FT-IR spectrum of LB-ZnO NPs suggests that the phytoconstituents of LB aqueous extracts were either degraded or remained absorbed in smaller quantities due to calcination of NPs at higher temperature [56]. The peak observed in the present study at 900 cm^{-1} are due to the asymmetrical and symmetrical stretching of the zinc carboxylate. Previous reports have disscussed that the spectral signatures of carboxylate impurities gets disappear as the calcination temperature increases indicating the possibility of zinc carboxylate dissociation and conversion to ZnO during the calcination process [57]. Absorption at 400 cm^{-1} to 600 cm^{-1} denotes the presence of ZnO NPs as metal oxide vibrational peaks [58]. We found the similar band at 570 cm^{-1} which could be ascribed to Zn–O stretching vibration of ZnO NPs [59] which can be seen in Fig. 2b and is absent in LB aqueous extract (Fig. 2a). It can, therefore, be supposed that the ZnO NPs is synthesized and stabilized by carboxyl, methyl and hydroxyl groups in the phytoconstituents of LB extract but after calcination, these organic molecules were degraded.

3.1.3 XRD analysis

XRD is a robust, non-destructive analytical tool used to classify and quantitatively evaluate various crystalline compounds. The XRD spectra of ZnO NPs synthesized with LB extract is illustrated in Fig. 3. X-ray diffraction peaks recorded at 31.75°, 34.52°, 36.23°, 47.53°, 56.58°, 62.84°, 66.24°, 67.92°, 69.04°, 72.65°, and 76.92° are attributed

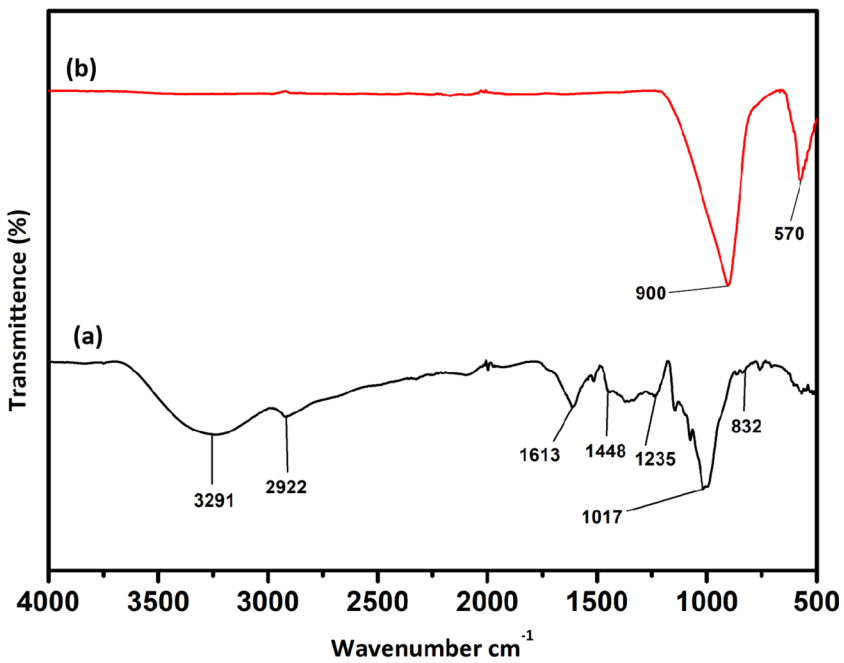

Fig. 2 FTIR spectrum of (*a*) *L. racemosa* flower buds extract. (*b*) Bio synthesized *L. racemosa* flower buds mediated ZnO NRs

to crystal planes of (100), (002), (101), (102), (110), (103), (200), (112), (201), (004) and (202) of synthesized LB-ZnO NPs, which corresponds to hexagonal wurtzite structural characteristics (JCPDS card number 36-1451, International Diffraction Data Center ver. 2002). Besides, no additional peaks in diffraction could be found in the XRD spectrum of LB-ZnO NPs suggesting complete decomposition of LB extract and zinc acetate precursor, without any other crystal impurities. Our findings are comparable with Narendhran and Shivaraj [60], who have developed ZnO NPs using the *Lantana aculeata* leaf extract and to Vanathi et al. [61], where ZnO NPs were synthesized using *Eichornia crassipes* leaf extract. The average crystalline size of synthesized ZnO NPs was calculated to be 30.321 nm using the Debey-Scherrer equation as follows [62].

$$D = \frac{k\lambda}{\beta \cos\theta} \quad (2)$$

where D is the crystalline size, K is the shape factor i.e. 0.94, λ is the X-Ray wavelength (1.5406 Å), β is Full Width at half maximum (FWHM) in radians and θ is the Bragg angle.

3.1.4 SEM and EDS analysis

The surface morphology and topography of the synthesized particles can be analyzed using SEM. In the present study, the SEM micrograph images (Fig. 4a, b) revealed the formation of zinc oxide nanorods with an average size of 250–300 nm. The resulting morphology of ZnO NRs was quite similar to earlier reported literature [63]. Rods with small morphology is usually preferred for the biomedical field while ZnO rods have better optical characteristics that can lead to significant pharmacological properties [64]. EDX spectrum revealed that there was a strong signal from the Zn atoms along with a low signal from the O atoms represented in Fig. 4c confirming ZnO NRs formation. Also, we found the presence of two small elemental peaks at around 9.5 and 8.5 keV ascribed to elemental zinc. Previous studies have reported major peaks at 1 to 10 keV in ZnO NPs synthesized using *Trifolium pratense* flower extract [65]. From the figure, we can observe the peaks of zinc and oxygen along with carbon, which may have come because of phytoconstituents from LB aqueous extract which acted as a capping agent to NPs. The figure also displays the major element as zinc which comprises more than 80% of total constituent along with oxygen, which further confirms the formation of pure ZnO NRs from LB extract.

3.1.5 TEM analysis

The TEM analysis of the synthesized LB-ZnO NPs is shown in Fig. 5. TEM micrographs of the produced nanoparticles at different magnifications are shown in Fig. 5a–c which clearly shows mixed morphology of ZnO NPs. Synthesized NPs were mostly rod-like structures with the average size in the range of 250–300 nm in length and 45–50 nm in diameter. Comparable results were found using *Myristica fragrans* leaves extract synthesized ZnO nanorods (ZnO NRs) with a range of 50–100 nm [66]. Another report demonstrated the synthesis of ZnO NRs using *Ricinus*

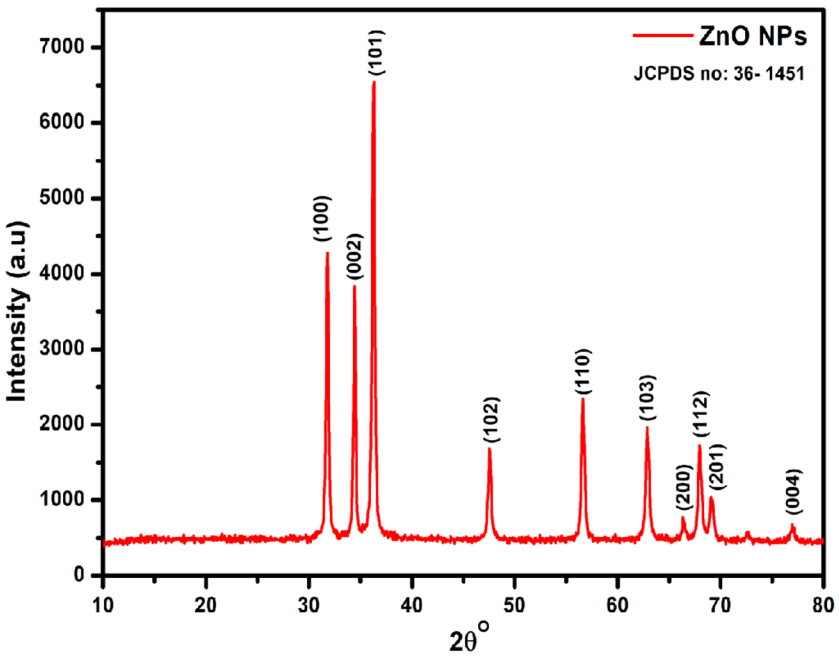

Fig. 3 X-ray diffraction analysis of zinc oxide nanorods biosynthesized using the *L. racemosa* flower buds extract

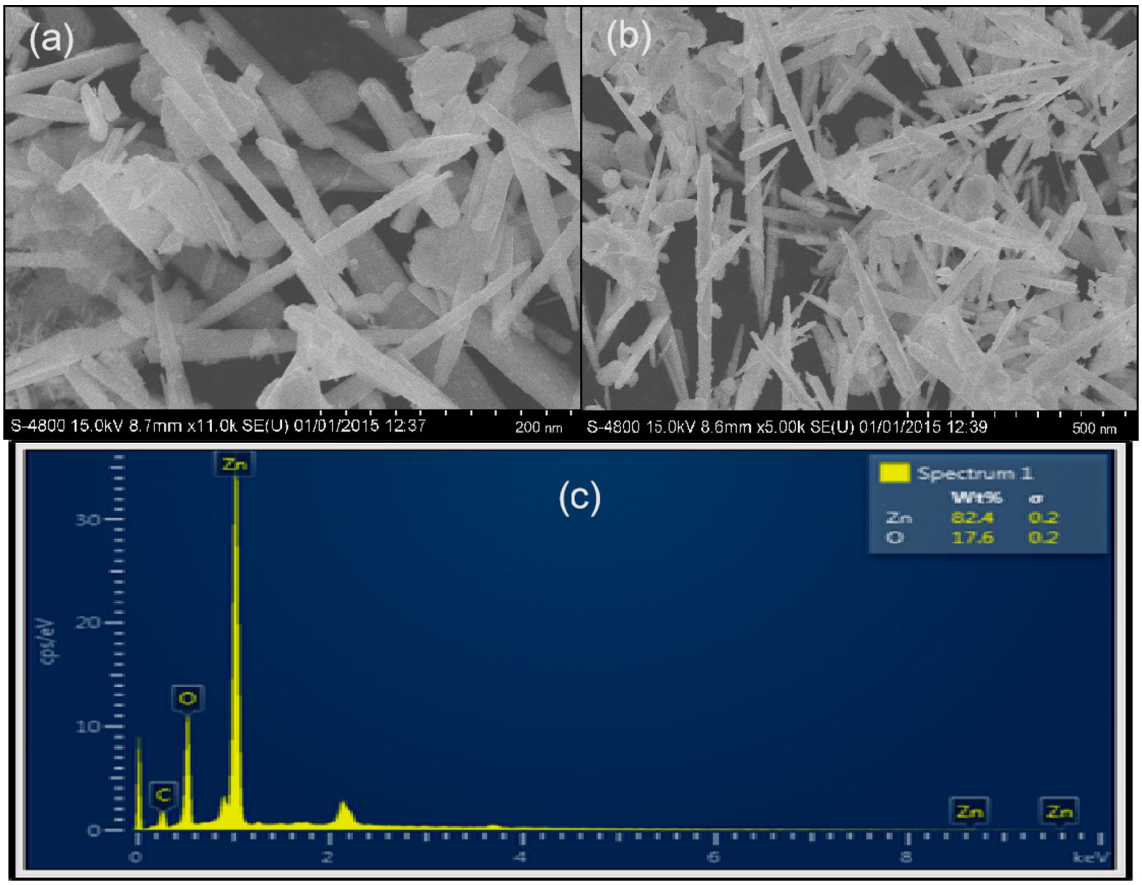

Fig. 4 **a**, **b** SEM image of ZnO nanorods synthesized from *L. racemosa* flower buds exact. **c** EDS analysis of ZnO nanorods biosynthesized using *L. racemosa* flower buds extract

communis L. leaf extract which had a diameter of 52.84 nm and length of 700 nm [67]. Figure 5e shows the selected area diffraction pattern (SAED) of *L. racemosa* flower buds fabricated ZnO NRs, corresponding to the hexagonal wurtzite structure of ZnO which correlates well with the XRD results.

3.1.6 Surface charge and stability by Zeta potential

The surface charge and stability of the synthesized LB-ZnO NRs was analysed by Zeta potential (ZP). Surface charge plays an important role in confirming the stability of NPs in a liquid medium. The zeta potential value for LB-ZnO NRs was around − 23.5 mV (Fig. 6) indicating a negative surface charge on synthesized NPs. Similar results were obtained by ZnO NRs synthesized using *Santalum album* leaf extract with zeta potential value of − 13 mV [68]. It should be noted that the particles with zeta potential values more positive than + 30 mV or more negative than − 30 mV are considered to be stable [69]. In contrast, the colloids are least stable at the isoelectric point, where the zeta potential is zero. The high negative value on synthesized LB-ZnO NRs confirms the repulsion among the particles and suggesting the synthesized NRs are stable.

3.2 Mosquito larvicidal activity

Different concentrations of LB extract and synthesized LB-ZnO NRs were tested on the early 4th instar larvae of *Ae. aegypti* for 24 h to evaluate their efficacy. Results indicate as the concentration of plant extracts and ZnO NRs increased the mortality of mosquito larvae increased. The LB aqueous extract was less toxic than synthesized LB-ZnO NRs against *Ae. aegypti*. 100% mortality was recorded by LB-ZnO NRs at 50 µg/ml with LC_{50} and LC_{90} values of 24.74 and 42.09 µg/ml respectively. While LB extract showed 100% mortality at 2500 µg/ml with LC_{50} and LC_{90} values of 1333.75 and 2216.48 µg/ml respectively (Table 1). Control did not show any toxicity to mosquito larvae and χ^2 value shows a significant difference at $p < 0.05$ level. Results indicate the larvicidal potential of LB-ZnO NRs being 50 folds more potent than LB extract. There are no reports on the larvicidal activity of ZnO NRs synthesized from *L. racemosa* plant but few mangroves have been screened

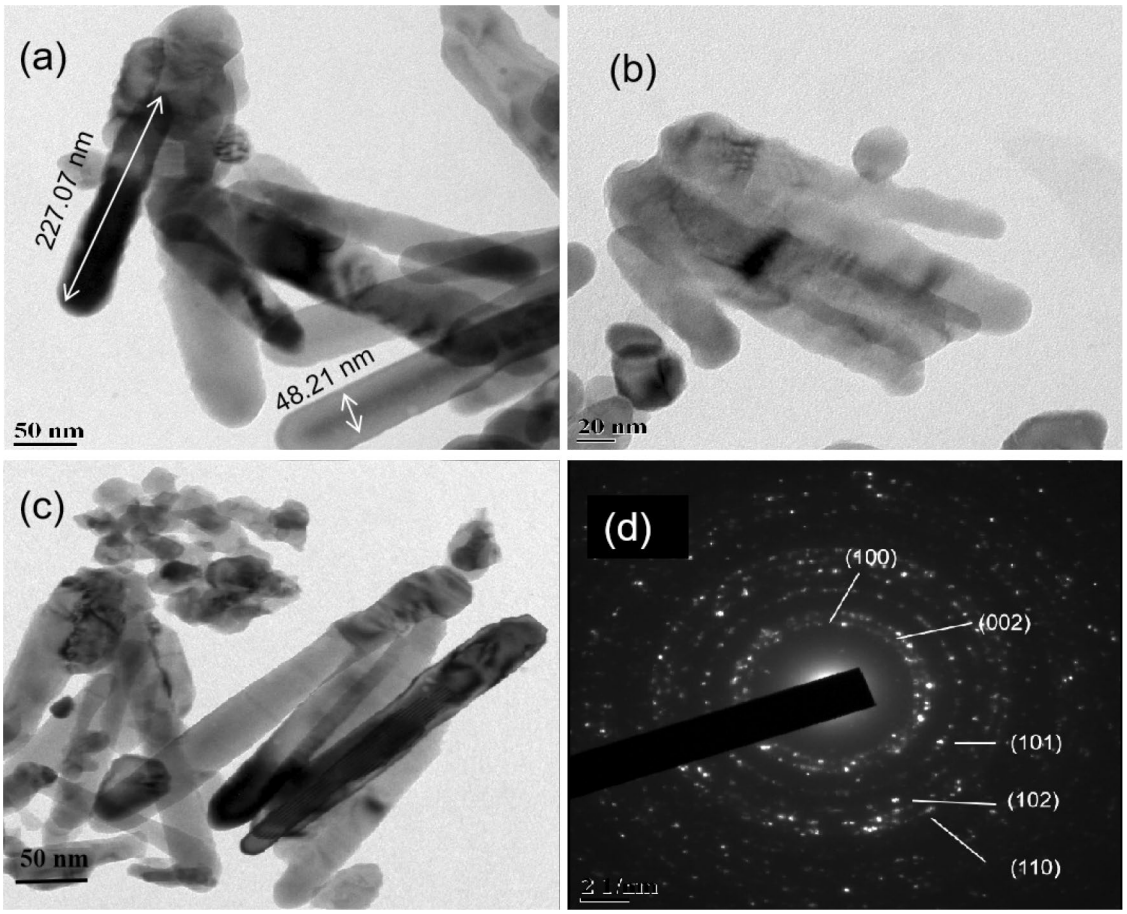

Fig. 5 **a**–**c** represents TEM images of bio-synthesized ZnO NRs using *L. racemosa* aqueous extract, **d** SAED pattern of synthesized ZnO NRs

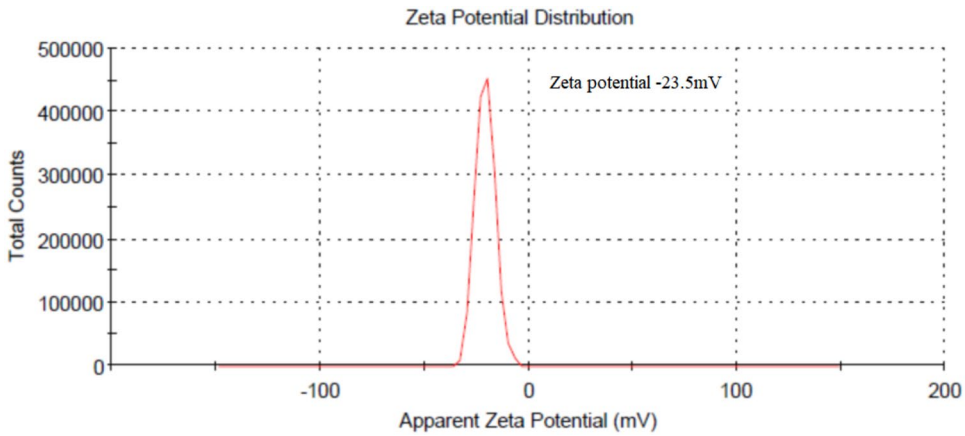

Fig. 6 Zeta potential of biosynthesized ZnO NRs in deionized water

for their larvicidal activity. Jisha and Shreeja [17] showed potential larvicidal activity against *Ae. aegypti* larvae by *L. racemosa* leaf acetone extract with an LC_{50} value of 8 mg/L. Similar results were also recorded by Ali et al. [70] in *E. agallocha* leaf ethanol extract on *Ae. aegypti* larvae with LC_{50} value of 67.1 mg/ml.

The mortality effect of LB-ZnO NRs on mosquito larvae can be attributed to the internal toxic effects of tiny particles inside the cuticle and the accumulation of LB-ZnO NRs in the alimentary canal. Also, small particles have been reported to target individual cells and interfere with moulting and other physiological processes which hinders the development of mosquito larvae [71]. Similar results

Table 1 Larvicidal toxicity of *L. racemosa* flower buds extract and synthesized ZnO nanorods against the dengue vector *Aedes aegypti*

Treatment	Concentration (µg/ml)	24 h mortality (%) ± SEM	LC_{50} (µg/ml)	LCL-UCL	LC_{90} (µg/ml)	LCL-UCL	χ^{2*} (d.f.)
L. racemosa flower buds aqueous extract	500	17.5 ± 1.44	1333.75	1104.59–1569.60	2216.48	1917.77–2741.08	12.57 (5) ($p = 0.014$)
	1000	33.34 ± 1.77					
	1500	54.16 ± 2.37					
	2000	78.75 ± 2.31					
	2500	99.16 ± 0.56					
Synthesized ZnO NRs	10	15.83 ± 1.82	24.74	20.22–29.23	42.09	36.41–51.85	12.17 (5) ($p = 0.016$)
	20	43.33 ± 2.77					
	30	62.91 ± 3.91					
	40	80.05 ± 7.68					
	50	100.00 ± 0.00					

Control group did not showed any mortality

LC_{50} lethal concentration (µg/ml) that kills 50% of the exposed organisms, LC_{90} lethal concentration (µg/ml) that kills 90% of the exposed organisms, χ^2 Chi square, *d.f.* degrees of freedom

*Significance at ($p \leq 0.05$)

were obtained by ZnO NRs synthesized using *Myristica fragrans* aqueous leaf extract and *Ulva lactuca*-fabricated ZnO NPs which was highly effective against *Ae. aegypti* 4th instar larvae [49, 66].

Mosquito larvicidal toxicity was further studied through morphological changes by exposing LB extract and LB-ZnO NRs at their highest concentration and visualizing affected larvae under the Stereo Zoom microscope (Fig. 7). On treatment with both LB extract and LB-ZnO NRs, *Ae. aegypti* larval body shrank and darkened which gave burnt like appearance. Besides, larvae treated with LB-ZnO NRs showed an accumulation of NRs in the alimentary canal and the respiratory region i.e., siphon. These morphological changes seem to be responsible for the larvicidal toxicity by LB extract and LB-ZnO NRs. Similar morphological damages were reported by Abinaya et al. [72] when *Ae. aegypti* larvae were treated with bacterial exopolysaccharide (EPS)-coated ZnO nanoparticles.

Overall the results suggest that mortality in larvae might be due to the accumulation of LB-ZnO NRs in the entire alimentary canal and in the siphon region.

3.3 Enzyme activity

3.3.1 Acetylcholinesterase activity

AChE is an enzyme involved in the hydrolysis of acetylcholine and its activity is inhibited by the tested compounds at nerve synapses and neuromuscular junctions. Many insecticide classes such as organophosphates and carbamates are responsible for inhibition of AChE irreversibly and causes insect mortality [73]. AChE enzyme was used as a surrogate biomarker to assess the neurotoxicity in vitro [74]. Given this, we carried out a study involving the effect of LB extract and LB-ZnO NRs on AChE activity of *Ae. aegypti* 4th instar larvae. The exposure of the larvae to LB extract and LB-ZnO NRs for 24 h significantly decreased the AChE activity to 2.42 µM ACT/mg/min and 1.41 µM ACT/mg/min respectively compared to the control value of 3.58 µM ACT/mg/min of homogenate (Fig. 8). This corresponds to 32% and 60.6% inhibition of AChE activity in larvae treated with LB extract and LB-ZnO NRs. Previous reports of mangroves plants viz. *Rhizophora apiculata, Rhizophora annamalayana, Rhizophora mucronata*, *Avicennia marina and Bruguiera cylindrica* showed 50% inhibition of AChE activity in mosquito larvae [75]. Extracts of *Sapindus emarginatus* showed comparable results to our study by altering the rates of AChE significantly in dengue larvae [76]. For biomonitoring studies and metal toxicity experiments on cholinesterases (ChEs), assessing the effect of metals on the activity of AChE has been a major challenge. Nevertheless, little work has been done to examine the interactions between AChE and metallic nanoparticles [77, 78]. There are no reports on the AChE inhibition in *Ae. aegypti* larvae by ZnO NRs using mangrove plant extracts. However silver nanoparticles synthesized using *Cassia fistula*-fruit pulp extract demonstrated lowered AChE activity of 62% in *Aedes albopictus* larvae [79]. Similarly, inhibition in AChE activity was observed by α-chitin nanoparticles, silver nanoparticles synthesized using shells of *Penaeus monodon Fabricius* and their nanocomposite when treated against *Ae. aegypti* larvae [80]. According to previous studies, it was found that toxic compounds affect the digestive system, the respiratory system and the nervous system in the larvae [81]. AChE enzyme inhibition causes the muscles to remain contracted leading to paralysis and finally

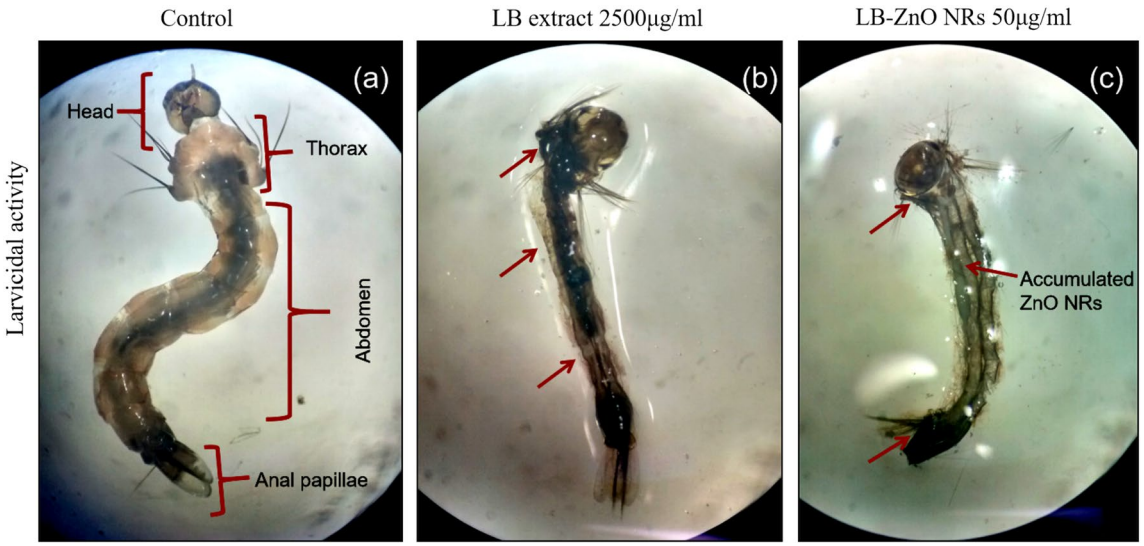

Fig. 7 Morphological changes in *Ae. aegypti* larvae after 24 h. **a** Control larvae after 24 h, **b** when exposed to *L. racemosa* flower buds extract **c** *L. racemosa* flower buds extract synthesized ZnO NRs. Arrow in red color (→) indicates the damages to head, abdominal region, thorax region and siphon

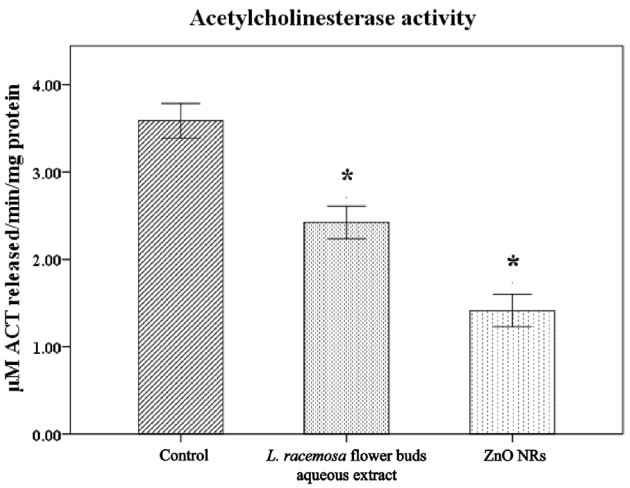

Fig. 8 Activity of acetylcholinesterase of *Ae. aegypti* larvae at LC_{50} concentration of *L. racemosa* flower buds aqueous extract and *L. racemosa* flower synthesized ZnO NRs. Results are presented as mean ± SEM (n = 3). *p < 0.05 (ANNOVA, Tukey's HSD test) denote significant difference compared to the control

death [82]. In the present study larvae exposed to LB aqueous extract and LB-ZnO NRs displayed tremors, rigidity and inability to reach the water surface when touched. These symptoms are suggestive of the respiratory muscles paralysis caused by LB-ZnO NRs due to AChE inhibition. This inhibition probably would have compromised the larval ability to breathe freely leading to death. Thus results under present studies indicate the neurotoxic potential of LB-ZnO NRs.

3.3.2 Glutathione S-transferase activity

GST normally plays an important role in detoxification of exogenous compounds. Compounds such as insecticides enter target insect tissues and organs and affect the activity of different detoxifying enzymes. Some compounds may inhibit the activity of GSTs, while others may enhance the activity of GSTs [83]. In this study, there was a slight increase in GST activity by LB extract (0.416 µM CDNB conjugated/min/mg protein) while significant decrease in GST activity was witnessed in larvae treated with LB-ZnO NRs (0.276 µM CDNB conjugated/min/mg protein) as compared to control (0.37 µM CDNB conjugated/min/mg protein) (Fig. 9). Thus 11% increment in GST activity in *Ae. aegypti* larvae when treated with LB aqueous extract signifies the larvae were trying to detoxify plant metabolites. In contrast, 25% reduction in GST activity by LB-ZnO NRs indicated that the ZnO NRs might be involved in a redox reaction and causes oxidative stress damage in the larval tissues [84–86]. A similar decrease in GST activity was shown by *Pongamia pinnata* leaf extract coated ZnO nanoparticles in *Callosobruchus maculatus* [28]. Thus inhibition or stimulation of these enzymes by insecticides can lead to metabolic inequalities, growth retardation and induction of mortality in mosquito larvae [87].

3.4 DNA fragmentation assay

The purity of DNA was recorded and the A260/A280 ratio was found to be 1.8–2.0 ± 0.05. LB aqueous extract displayed slight but significant damage to the *Ae.*

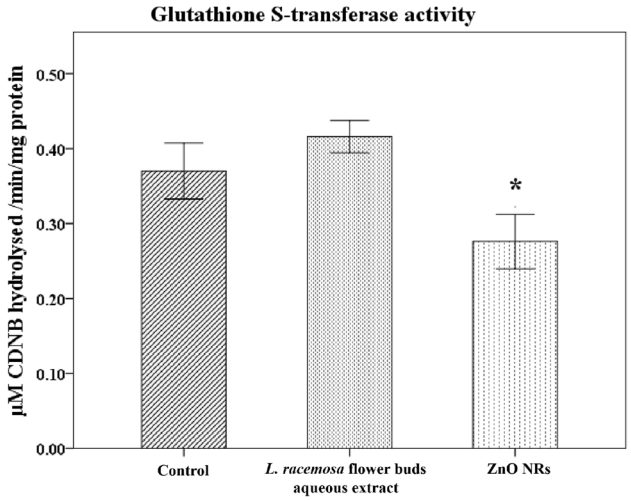

Fig. 9 Activity of Glutathione S- transferase of *Ae. aegypti* larvae treated at LC_{50} concentration of *L. racemosa* flower buds aqueous extract and *L. racemosa* flower synthesized ZnO NRs. Results are presented as mean ± SEM (n = 3). *p < 0.05 (ANNOVA, Tukey's HSD test) denote significant difference compared to the control

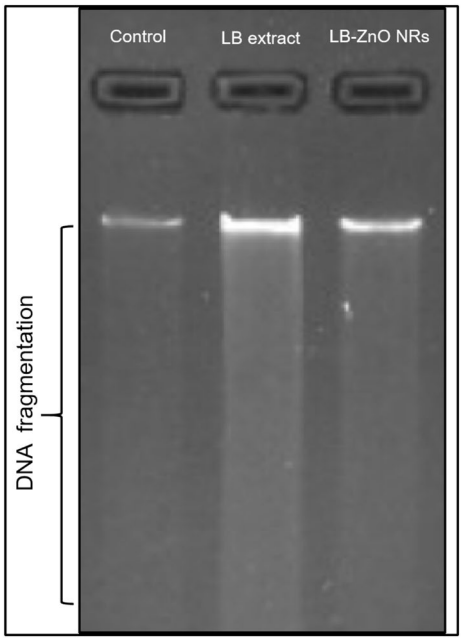

Fig. 10 DNA fragmentation assay of *Ae. aegypti* larvae treated with *L. racemosa* flower buds aqueous extract (LB) and *L. racemosa* flower synthesized ZnO NRs (LB-ZnO NRs) as compared to control

aegypti larval DNA as compared to LB-ZnO NRs and control-treated larval DNA (Fig. 10). This indicates that synthesized LB-ZnO NRs do not demonstrate any nicking activity in mosquito DNA confirming the mortality of larvae is based solely on cytotoxicity and can be used as a safe alternative to commercial insecticides in the field.

4 Conclusion

This study reports for the first time green synthesis of zinc oxide nanorods using *L. racemosa* flower buds. The characterization results recorded from UV–Vis spectrophotometry, TEM, SEM, XRD, FTIR and EDX analyses support the effective biosynthesis of *L. racemosa* flower buds extract fabricated ZnO NRs. The synthesized LB-ZnO NRs are crystalline with an average length of 250–300 nm and 40–50 nm in diameter. Present research highlighted that the ZnO NRs are easy to produce, and can be employed at low dosages to strongly reduce populations of the dengue vector, *Ae. aegypti* with LC_{50} at 24.74 µg/ml. Besides, LB-ZnO NRs also affected the activity of enzymes in *Ae. aegypti* larvae, which demonstrated decreased AChE and GST activity, responsible for signal transduction and resistivity of xenobiotics with no genetic impairment. The study concludes that LB-ZnO NRs can be used as an efficient nanobiopesticides for controlling dengue vector *Ae. aegypti* larvae in the future.

Acknowledgements Authors are thankful to the Department of Life Sciences, Department of Chemistry, National Centre for Nanoscience and Nanotechnology, University of Mumbai; IIT Bombay (SAIF) for accessing Instrument Facility. Department of Zoonosis, Haffkine Institute for Training Research & Testing Mumbai, Maharashtra for identification of Mosquito species.

Compliance with ethical standards

Conflict of interest Authors declare no conflict of interest.

References

1. Benelli G, Mehlhorn H (2016) Declining malaria, rising of dengue and Zika virus: insights for mosquito vector control. Parasitol Res 115(5):1747–1754. https://doi.org/10.1007/s00436-016-4971-z
2. World Health Organization (2012) Handbook for integrated vector management. World Health Organization, Geneva
3. Veerakumar K, Govindarajan M, Rajeswary M, Muthukumaran U (2014) Mosquito larvicidal properties of silver nanoparticles synthesized using *Heliotropium indicum* (Boraginaceae) against *Aedes aegypti*, *Anopheles stephensi* and *Culex quinquefasciatus* (Diptera: Culicidae). Parasitol Res 113(6):2363–2373. https://doi.org/10.1007/s00436-014-3895-8
4. Benelli G, Romano D (2017) Mosquito vectors of Zika virus. Entomol Gener. https://doi.org/10.1127/entomologia/2017/0496
5. Harrington LC, Scott TW, Lerdthusnee K, Coleman RC, Costero A, Clark GG, Jones JJ, Kitthawee S, Kittayapong P, Sithiprasasna R, Edman JD (2005) Dispersal of the dengue vector *Aedes aegypti* within and between rural communities. Am J Trop Med Hyg 72(2):209–220. https://doi.org/10.4269/ajtmh.2005.72.209

6. Murugan K, Hwang JS, Kovendan K, Kumar KP, Vasugi C, Kumar AN (2011) Use of plant products and copepods for control of the dengue vector, *Aedes aegypti*. Hydrobiologia 666:331–338. https://doi.org/10.1007/s10750-011-0629-0
7. De Castro BM, De Jaeger X, Martins-Silva C, Lima RD, Amaral E, Menezes C, Lima P, Neves CM, Pires RG, Gould TW, Welch I (2009) The vesicular acetylcholine transporter is required for neuromuscular development and function. Mol Cell Biol 29(19):5238–5250. https://doi.org/10.1128/MCB.00245-09
8. Melo-Santos MA, Varjal-Melo JJ, Araújo AP, Gomes TC, Paiva MH, Regis LN, Furtado AF, Magalhaes T, Macoris ML, Andrighetti MT, Ayres CF (2010) Resistance to the organophosphate temephos: mechanisms, evolution and reversion in an *Aedes aegypti* laboratory strain from Brazil. Acta Trop 113(2):180–189. https://doi.org/10.1016/j.actatropica.2009.10.015
9. Benelli G (2015) Research in mosquito control: current challenges for a brighter future. Parasitol Res 114(8):2801–2805. https://doi.org/10.1007/s00436-015-4586-9
10. Fillinger U, Lindsay SW (2011) Larval source management for malaria control in Africa: myths and reality. Malaria J 10(353):1–10. https://doi.org/10.1186/1475-2875-10-353
11. Azizullah A, Rehman ZU, Ali I, Murad W, Muhammad N, Ullah W, Häder DP (2014) Chlorophyll derivatives can be an efficient weapon in the fight against dengue. Parasitol Res 113(12):4321–4326. https://doi.org/10.1007/s00436-014-4175-3
12. De Lacerda LD, Jose DV, De Rezende CE, Maria Cristina F, Wasserman JC, Martins JC (1986) Leaf chemical characteristics affecting herbivory in a New World mangrove forest. Biotropica 18:350–355
13. Anjaneyulu M, Chopra K (2003) Quercetin, a bioflavonoid, attenuates thermal hyperalgesia in a mouse model of diabetic neuropathic pain. Prog Neuropsychopharmacol Biol Psychiatry 27(6):1001–1005. https://doi.org/10.1016/S0278-5846(03)00160-X
14. DeSouza L, Wahidullah S (2010) Antibacterial phenolics from the mangrove *Lumnitzera racemosa*. Indian J Mar Sci 39(2):294–298
15. Lin TC, Hsu FL, Cheng JT (1993) Antihypertensive activity of corilagin and chebulinic acid, tannins from *Lumnitzera, racemosa*. J Nat Prod 56(4):629–632. https://doi.org/10.1021/np50094a030
16. Ravikumar S, Gnanadesigan M (2011) Hepatoprotective and antioxidant activity of a mangrove plant *Lumnitzera racemosa*. Asian Pac J Trop Biomed 1(5):348–352. https://doi.org/10.1016/S2221-1691(11)60078-6
17. Jisha S, Sreeja J (2018) Preliminary study on the mosquito larvicidal efficacy of mangrove leaf extracts. Indian J Sci Res 20(1):68–70
18. Lardeux F, Rivière F, Sechan Y, Loncke S (2002) Control of the Aedes vectors of the dengue viruses and *Wuchereria bancrofti*: the French Polynesian experience. Ann Trop Med Parasitol 96(2):105–116. https://doi.org/10.1179/000349802125002455
19. Banumathi B, Vaseeharan B, Ishwarya R, Govindarajan M, Alharbi NS, Kadaikunnan S et al (2017) Toxicity of herbal extracts used in ethno-veterinary medicine and green-encapsulated ZnO nanoparticles against *Aedes aegypti* and microbial pathogens. Parasitol Res 116(6):1637–1651. https://doi.org/10.1007/s00436-017-5438-6
20. Murugan K, Benelli G, Panneerselvam C, Subramaniam J, Jeyalalitha T, Dinesh D et al (2015) *Cymbopogon citratus*-synthesized gold nanoparticles boost the predation efficiency of copepod *Mesocyclops aspericornis* against malaria and dengue mosquitoes. Exp Parasitol 153:129–138. https://doi.org/10.1016/j.exppara.2015.03.017
21. Ishwarya R, Vaseeharan B, Anuradha R, Rekha R, Govindarajan M, Alharbi NS et al (2017) Eco-friendly fabrication of Ag nanostructures using the seed extract of *Pedalium murex*, an ancient Indian medicinal plant: Histopathological effects on the Zika virus vector *Aedes aegypti* and inhibition of biofilm-forming pathogenic bacteria. J Photochem Photobiol B 174:133–143. https://doi.org/10.1016/j.jphotobiol.2017.07.026
22. Sirelkhatim A, Mahmud S, Seeni A, Kaus NH, Ann LC, Bakhori SK, Hasan H, Mohamad D (2015) Review on zinc oxide nanoparticles: antibacterial activity and toxicity mechanism. Nano-Micro Lett 7(3):219–242. https://doi.org/10.1007/s40820-015-0040-x
23. Fortunato EM, Barquinha PM, Pimentel AC, Gonçalves AM, Marques AJ, Pereira LM, Martins RF (2005) Fully transparent ZnO thin-film transistor produced at room temperature. Adv Mater 17(5):590–594. https://doi.org/10.1002/adma.200400368
24. Loan TT, Long NN (2009) Photoluminescence properties of Co-doped ZnO nanorods synthesized by hydrothermal method. J Phys D 42(6):065412. https://doi.org/10.1088/0022-3727/42/6/065412
25. Nie L, Gao L, Feng P, Zhang J, Fu X, Liu Y, Yan X, Wang T (2006) Three-dimensional functionalized tetrapod-like ZnO nanostructures for plasmid DNA delivery. Small 2(5):621–625. https://doi.org/10.1002/smll.200500193
26. Yoon SH, Kim DJ (2006) Fabrication and characterization of ZnO films for biological sensor application of FPW device. In: Proceedings of the 2006 15th IEEE international symposium on the applications of ferroelectrics Jul 30, 322–325. IEEE.
27. Xiong HM (2013) ZnO nanoparticles applied to bioimaging and drug delivery. Adv Mater 25(37):5329–5335. https://doi.org/10.1002/adma.201301732
28. Malaikozhundan B, Vaseeharan B, Vijayakumar S, Pandiselvi K, Kalanjiam MAR, Murugan K, Benelli G (2017) Biological therapeutics of *Pongamia pinnata* coated zinc oxide nanoparticles against clinically important pathogenic bacteria, fungi and MCF-7 breast cancer cells. Microb Pathog 104:268–277. https://doi.org/10.1016/j.micpath.2017.01.029
29. Applerot G, Lipovsky A, Dror R, Perkas N, Nitzan Y, Lubart R, Gedanken A (2009) Enhanced antibacterial activity of nanocrystalline ZnO due to increased ROS-mediated cell injury. Adv Func Mater 19(6):842–852. https://doi.org/10.1002/adfm.200801081
30. Sharma D, Rajput J, Kaith BS, Kaur M, Sharma S (2010) Synthesis of ZnO nanoparticles and study of their antibacterial and antifungal properties. Thin Solid Films 519(3):1224–1229. https://doi.org/10.1016/j.tsf.2010.08.073
31. Kirthi AV, Rahuman AA, Rajakumar G, Marimuthu S, Santhoshkumar T, Jayaseelan C, Velayutham K (2011) Acaricidal, pediculocidal and larvicidal activity of synthesized ZnO nanoparticles using wet chemical route against blood feeding parasites. Parasitol Res 109(2):461–472. https://doi.org/10.1007/s00436-011-2277-8
32. Kumar S, Warikoo R, Wahab N (2010) Larvicidal potential of ethanolic extracts of dried fruits of three species of peppercorns against different instars of an Indian strain of dengue fever mosquito, *Aedes aegypti* L. (Diptera: Culicidae). Parasitol Res 107(4):901–907. https://doi.org/10.1007/s00436-010-1948-1
33. Finlayson C, Saingamsook J, Somboon P (2015) A simple and affordable membrane-feeding method for *Aedes aegpyti* and *Anopheles minimus* (Diptera: Culicidae). Acta Trop 152:245–251. https://doi.org/10.1016/j.actatropica.2015.09.026
34. Zaim M/WHOPES (2005) https://www.who.int/whopes/resources/who_cds_whopes_gcdpp_2005.13/en/
35. Coelho JS, Santos NDL, Napoleao TH, Gomes FS, Ferreira RS, Zingali RB, Coelho LCBB, Leite SP, Navarro DMAF, Paiva PMG (2009) Effect of *Moringa oleifera* lectin on development and mortality of *Aedes aegypti* larvae. Chemosphere 77:934–938. https://doi.org/10.1016/j.ecoenv.2017.01.026
36. Napoleão TH, Pontual EV, de Albuquerque TL, de Lima Santos ND, Sá RA, Coelho LCCB et al (2012) Effect of *Myracrodruon urundeuva* leaf lectin on survival and digestive enzymes of

Aedes aegypti larvae. Parasitol Res 110(2):609–616. https://doi.org/10.1007/s00436-011-2529-7
37. Bradford MM (1976) A rapid and sensitive method for the quantitation of microgram quantities of protein utilizing the principle of protein-dye binding. Anal Biochem 72(1–2):248–254. https://doi.org/10.1016/0003-2697(76)90527-3
38. Ellman GL, Courtney KD Jr, Andres V, Featherstone RM (1961) A new and rapid colorimetric determination of acetylcholinesterase activity. Biochem Pharmacol 7(2):88–95. https://doi.org/10.1016/0006-2952(61)90145-9
39. Ikezawa H, Taguchi R (1981) Phosphatidylinositol-specific phospholipase C from *Bacillus cereus* and *Bacillus thuringiensis*. Methods Enzymol 71:731–741. https://doi.org/10.1016/0076-6879(81)71086-3
40. Vontas JG, Enayati AA, Small GJ, Hemingway J (2000) A simple biochemical assay for glutathione S-transferase activity and its possible field application for screening glutathione S-transferase-based insecticide resistance. Pestic Biochem Physiol 68(3):184–192. https://doi.org/10.1006/pest.2000.2512
41. Habig WH, Pabst MJ, Jakoby WB (1974) Glutathione S-transferases the first enzymatic step in mercapturic acid formation. J Biol Chem 249(22):7130–7139
42. Rajasekharreddy P, Rani PU (2014) Biofabrication of Ag nanoparticles using *Sterculia foetida* L. seed extract and their toxic potential against mosquito vectors and HeLa cancer cells. Mater Sci Eng C 39:203–212. https://doi.org/10.1016/j.msec.2014.03.003
43. Gupta S, Preet S (2012) Protocol optimization for genomic DNA extraction and RAPD-PCR in mosquito larvae (Diptera: Culicidae). Ann Biol Res 3(3):1553–1561
44. Glasel JA (1995) Validity of nucleic acid purities monitored by 260nm/280nm absorbance ratios. Biotechniques 18(1):62–63
45. Rajesh WR, Jaya RL, Niranjan SK, Vijay DM, Sahebrao BK (2009) Phytosynthesis of Silver Nanoparticle Using *Gliricidia sepium* (Jacq.). Curr Nanosci 5:117–122. https://doi.org/10.2174/1573413309787314674
46. Zak AK, Majid WHA, Mahmoudian MR, Darroudi M, Youse R (2013) Starch-stabilized synthesis of ZnO nanopowders at low temperature and optical properties study. Adv Powder Technol 24:618–624. https://doi.org/10.1016/j.apt.2012.11.008
47. Zak AK, Abrishami ME, Majid WA, Yousefi R, Hosseini SM (2011) Effects of annealing temperature on some structural and optical properties of ZnO nanoparticles prepared by a modified sol–gel combustion method. Ceram Int 37(1):393–398. https://doi.org/10.1016/j.ceramint.2010.08.017
48. Mahamuni PP, Patil PM, Dhanavade MJ, Badiger MV, Shadija PG, Lokhande AC, Bohara RA (2019) Synthesis and characterization of zinc oxide nanoparticles by using polyol chemistry for their antimicrobial and antibiofilm activity. Biochem Biophys Rep 17:71–80. https://doi.org/10.1016/j.bbrep.2018.11.007
49. Ishwarya R, Vaseeharan B, Kalyani S, Banumathi B, Govindarajan K, Alharbi NS, Kadaikunnan S, Al-anbr MN, Khaled JM, Benelli G (2018) Facile green synthesis of zinc oxide nanoparticles using *Ulva lactuca* seaweed extract and evaluation of their photocatalytic, antibiofilm and insecticidal activity. J Photochem Photobiol B 178:249–258. https://doi.org/10.1016/j.jphotobiol.2017.11.006
50. Senthilkumar N, NandhaKumar E, Priya P, Soni D, Vimalan M, Potheher IV (2017) Synthesis of ZnO nanoparticles using leaf extract of *Tectona grandis* (L.) and their anti-bacterial, anti-arthritic, anti-oxidant and in vitro cytotoxicity activities. New J Chem 41:10347–10356. https://doi.org/10.1039/C7NJ02664A
51. Davis K, Yarbrough R, Froeschle M, White J, Rathnayake H (2019) Band gap engineered zinc oxide nanostructures via a sol–gel synthesis of solvent driven shape-controlled crystal growth. RSC Adv 9(26):14638–14648. https://doi.org/10.1039/C9RA02091H
52. Awwad AM, Salem NM, Abdeen AO (2012) Biosynthesis of Silver nanoparticles using *Olea europaea* leaves extract and its antibacterial activity. Nanosci Nanotechnol 2(6):164–170. https://doi.org/10.5923/j.nn.20120206.03
53. Zhang G, Du M, Li Q, Li X, Huang J, Jiang X, Sun D (2013) Green synthesis of Au–Ag alloy nanoparticles using *Cacumen platycladi* extract. Rsc Adv 3(6):1878–1884. https://doi.org/10.1039/C2RA22442A
54. Al RN, Al-Haidari KS (2016) Environmental friendly synthesis of silver nanoparticles using leaf extract of Mureira Tree (*Azadirachta indica*) cultivated in Iraq and efficacy the antimicrobial activity. J Nat Sci Res 6(4):2224–3186
55. Shankar SS, Ahmad A, Sastry M (2003) Geranium leaf assisted biosynthesis of silver nanoparticles. Biotechnol Prog 19(6):1627–1631. https://doi.org/10.1021/bp034070w
56. Bala N, Saha S, Chakraborty M, Maiti M, Das S, Basub R, Nandy P (2015) Green synthesis of zinc oxide nanoparticles using *Hibiscus subdariffa* leaf extract: effect of temperature on synthesis, anti-bacterial activity and anti-diabetic activity. RSC Adv 5:4993–5003. https://doi.org/10.1039/C4RA12784F
57. Xiong G, Pal U, Serrano JG, Ucer KB, Williams RT (2006) Photoluminesence and FTIR study of ZnO nanoparticles: the impurity and defect perspective. Phys Stat Solidi C 3(10):3577–3581. https://doi.org/10.1002/pssc.200672164
58. Yuvakkumar R, Suresh J, Saravanakumar B, Nathanael AJ, Hong SI, Rajendran V (2015) Rambutan peels promoted biomimetic synthesis of bioinspired zinc oxide nanochains for biomedical applications. Spectrochim Acta A 137:250–258. https://doi.org/10.1016/j.saa.2014.08.022
59. Ramesh AV, Pavankumar Y, Lavakusa B (2017) A facile green synthesis of ZnO nanorods using leaf extract of *Ficus hispida* L. Int J Eng Appl Sci Technol 2(4):2143
60. Narendhran S, Sivaraj R (2016) Biogenic ZnO nanoparticles synthesized using *L. aculeata* leaf extract and their antifungal activity against plant fungal pathogens. Bull Mater Sci 39:1–5. https://doi.org/10.1007/s12034-015-1136-0
61. Vanathi P, Rajiv P, Narendhran S, Rajeshwari S, Rahman PKSM, Venckatesh R (2014) Biosynthesis and characterization of phyto mediated zinc oxide nanoparticles: a green chemistry approach. Mater Lett 134:13–15. https://doi.org/10.1016/j.matlet.2014.07.029
62. Elango G, Roopan SM, Dhamodaran KI, Elumalai K, Al-dhabi NA, Arasu MV (2016) Spectroscopic investigation of biosynthesized nickel nanoparticles and its larvicidal, pesticidal activities. J Photochem Photobiol B 162:162–167. https://doi.org/10.1016/j.jphotobiol.2016.06.045
63. Zheng J, Nagashima K, Parmiter D, De Cruz J, Patri AK (2011) SEM X-Ray microanalysis of nanoparticles present in tissue or cultured cell thin sections. Methods Mol Biol 697:93–99. https://doi.org/10.1016/j.chemosphere.2009.08.022
64. Kim SJ, Park DW (2009) Preparation of ZnO nanopowders by thermal plasma and characterization of photo-catalytic property. Appl Surf Sci 255:5363–5367. https://doi.org/10.1016/j.apsusc.2008.10.028
65. Dobrucka R, Długaszewska J (2016) Biosynthesis and antibacterial activity of ZnO nanoparticles using *Trifolium pratense* flower extract. Saudi J Biol Sci 23(4):517–523. https://doi.org/10.1016/j.sjbs.2015.05.016
66. Ashokan AP, Paulpandi M, Dinesh D, Murugan K, Vadivalagan C, Benelli G (2017) Toxicity on dengue mosquito vectors through *Myristica fragrans* synthesized zinc oxide nanorods, and their cytotoxic effects on liver cancer cells (HepG2). J Clust Sci 28(1):205–226. https://doi.org/10.1007/s10876-016-1075-y
67. Chennimalai M, Do JY, Kang M, Senthil TS (2019) A facile green approach of ZnO NRs synthesized via *Ricinus communis* L leaf

extract for Biological activities. Mater Sci Eng C 103:109844. https://doi.org/10.1016/j.msec.2019.109844
68. Kavithaa K, Paulpandi M, Ponraj T, Murugan K, Sumathi S (2016) Induction of intrinsic apoptotic pathway in human breast cancer (MCF-7) cells through facile biosynthesized zinc oxide nanorods. Karbala Int J Mod Sci 2(1):46–55. https://doi.org/10.1016/j.kijoms.2016.01.002
69. Saeb A, Alshammari AS, Al-Brahim H, Al-Rubeaan KA (2014) Production of silver nanoparticles with strong and stable antimicrobial activity against highly pathogenic and multidrug resistant bacteria. Sci World J. https://doi.org/10.1155/2014/704708
70. Ali MS, Ravikumar S, Beula JM (2012) Spatial and temporal distribution of mosquito larvicidal compounds in mangroves. Asian Pac J Trop Dis 2(5):401–404. https://doi.org/10.1016/S2222-1808(12)60087-5
71. Murugan K, Anitha J, Suresh U, Rajaganesh R, Panneerselvam C, Tseng LC, Kalimuthu K, Alsalhi MS, Devanesan S, Nicoletti M, Sarkar SK (2017) Chitosan-fabricated Ag nanoparticles and larvivorous fishes: a novel route to control the coastal malaria vector *Anopheles sundaicus*? Hydrobiologia 797(1):335–350. https://doi.org/10.1007/s10750-017-3196-1
72. Abinaya M, Vaseeharan B, Divya M, Sharmili A, Govindarajan M, Alharbi NS, Kadaikunnan S, Khaled JM, Benelli G (2018) Bacterial exopolysaccharide (EPS)-coated ZnO nanoparticles showed high antibiofilm activity and larvicidal toxicity against malaria and Zika virus vectors. J Trace Elem Med Biol 45:93–103. https://doi.org/10.1016/j.jtemb.2017.10.002
73. Fournier D (2005) Mutations of acetylcholinesterase which confer insecticide resistance in insect populations. Chem Biol Interact 157–158:257–261. https://doi.org/10.1016/j.cbi.2005.10.040
74. Gupta VK, Pal R, Siddiqi NJ, Sharma B (2015) Acetylcholinesterase from human erythrocytes as a surrogate biomarker of lead induced neurotoxicity. Enzym Res 2015:1–7. https://doi.org/10.1155/2015/370705
75. Suganthy N, Pandian SK, Devi KP (2009) Cholinesterase inhibitory effects of *Rhizophora lamarckii*, *Avicennia officinalis*, *Sesuvium portulacastrum* and *Suaeda monica*: mangroves inhabiting an Indian coastal area (Vellar Estuary). J Enzym Inhib Med Chem 24(3):702–707. https://doi.org/10.1080/14756360802334719
76. Koodalingam A, Mullainadhan P, Arumugam M (2011) Effects of extract of soapnut *Sapindus emarginatus* on esterases and phosphatases of the vector mosquito, *Aedes aegypti* (Diptera: Culicidae). Acta Trop 118(1):27–36. https://doi.org/10.1016/j.actatropica.2011.01.003
77. Wang Z, Zhao J, Li F, Gao D, Xing B (2009) Adsorption and inhibition of acetylcholinesterase by different nanoparticles. Chemosphere 77:67–73. https://doi.org/10.1016/j.chemosphere.2009.05.015
78. Wang Z, Zhang K, Zhao J, Liu X, Xing B (2010) Adsorption and inhibition of butyrylcholinesterase by different engineered nanoparticles. Chemosphere 79:86–92. https://doi.org/10.1016/j.chemosphere.2009.12.051
79. Fouad H, Hongjie L, Hosni D, Wei J, Abbas G, Ga'alJianchu HM (2018) Controlling *Aedes albopictus* and *Culex pipiens pallens* using silver nanoparticles synthesized from aqueous extract of *Cassia fistula* fruit pulp and its mode of action. Artif Cells Nanomed Biotechnol 46(3):558–567. https://doi.org/10.1080/21691401.2017.1329739
80. Solairaj D, Rameshthangam P (2017) Silver nanoparticle embedded α-chitin nanocomposite for enhanced antimicrobial and mosquito larvicidal activity. J Polym Environ 25:435–452. https://doi.org/10.1007/s10924-016-0822-3
81. Lu FC, Kacew S (2002) Lus basic toxicology: fundamentals, targets organ and risk assesment, 4th edn. CRC Press, Boca Raton, pp 386–392
82. Kim IH, Suzuki R, Hitotsuyanagi Y, Takeya K (2003) Three novel quassinoids, javanicolides A and B, and javanicoside A, from seeds of *Brucea javanica*. Tetrahedron 59(50):9985–9989. https://doi.org/10.1016/j.tet.2003.10.048
83. Vanhaelen N, Haubruge E, Lognay G, Francis F (2001) Hoverfly glutathione S-transferases and effect of Brassicaceae secondary metabolites. Pestic Biochem Physiol 71(3):170–177. https://doi.org/10.1006/pest.2001.2573
84. Parkes TL, Hilliker AJ, Phillips JP (1993) Genetic and biochemical analysis of glutathione-S-transferase in the oxygen defense system of *Drosophila melanogaster*. Genome 36:1007–1014. https://doi.org/10.1139/g93-134
85. Giordano G, Afsharinejad Z, Guizzetti M, Vitalone A, Kavanagh TJ, Costa LG (2007) Organophosphorus insecticides chlorpyrifos and diazinon and oxidative stress in neuronal cells in a genetic model of glutathione deficiency. Toxicol Appl Pharmacol 219:181–189. https://doi.org/10.1016/j.taap.2006.09.016
86. Vontas JG, Graham J, Hemingway J (2001) Glutathione S-transferases as antioxidant defence agents confer pyrethroid resistance in *Nilaparvata lugens*. Biochem J 357:65–72. https://doi.org/10.1042/bj3570065
87. Vorbrodt A (1959) The role of phosphatase in intracellular metabolism. Postepy Hig Med Dosw 13:200–206